Pre-existence and emergence of drug resistance in a generalized model of intra-host viral dynamics

Epidemics 4 (2012) 187–202

Contents lists available at SciVerse ScienceDirect

Epidemics

journal homepage: www.elsevier.com/locate/epidemics

Pre-existence and emergence of drug resistance in a generalized model of intra-host viral dynamics

Helen K. Alexander*, Sebastian Bonhoeffer

Institute for Integrative Biology, ETH Zürich, Universitätsstrasse 16, CH-8092 Zürich, Switzerland

ARTICLE INFO

Article history:
Received 6 July 2012
Received in revised form 15 October 2012
Accepted 16 October 2012
Available online 24 October 2012

Keywords:
HIV
Hepatitis B
Hepatitis C
Evolutionary rescue
Life cycle
Stochastic process

ABSTRACT

Understanding the source of drug resistance emerging within a treated patient is an important problem, from both clinical and basic evolutionary perspectives. Resistant mutants may arise de novo either before or after treatment is initiated, with different implications for prevention. Here we investigate this problem in the context of chronic viral diseases, such as human immunodeficiency virus (HIV) and hepatitis B and C viruses (HBV and HCV). We present a unified model of viral population dynamics within a host, which can capture a variety of viral life cycles. This allows us to identify which results generalize across various viral diseases, and which are sensitive to the particular virus's life cycle. Accurate analytical approximations are derived that allow for a solid understanding of the parameter dependencies in the system. We find that the mutation-selection balance attained prior to treatment depends on the step at which mutations occur and the viral trait that incurs the cost of resistance. Life cycle effects and key parameters, including mutation rate, infected cell death rate, cost of resistance, and drug efficacy, play a role in determining when mutations arising during treatment are important relative to those pre-existing.

Introduction

Over the past two decades, the advent of highly effective antiviral drugs has revolutionized the treatment of chronic viral diseases, including human immunodeficiency virus (HIV) and hepatitis B and C viruses (HBV and HCV). These drugs have been successful in substantially reducing morbidity, mortality and transmission, but unfortunately they also impose a strong selection pressure, which has led to observations of drug resistance and associated treatment failure (Hirsch et al., 2008; Johnson et al., 2011). The emergence of drug resistance can be attributed to the remarkable potential of these viruses for rapid adaptation, due to characteristics such as a large population size, fast replication and a high mutation rate. The rapid accumulation of genetic diversity has the important consequence that many drug-resistant mutants are likely to exist already by the time treatment begins (Coffin, 1995). More generally, it has been pointed out that drug resistance may emerge from two sources: mutants pre-existing when treatment starts, or those generated de novo during residual replication under treatment (Ribeiro and Bonhoeffer, 2000). Distinguishing between these two sources of resistance has implications for treatment strategies. Treatment failure due to de novo mutants could be curtailed by a higher drug dose, minimizing ongoing replication of the drug-sensitive strain. The selection of pre-existing mutants, on the other hand, could be better avoided by combination therapy to which fewer mutants are resistant (Ribeiro and Bonhoeffer, 2000).

The source of resistance is, however, difficult to infer clinically. The detection of minority variants is limited by the extent of sampling and by the sensitivity of assays, making it challenging to detect rare variants and pinpoint when mutants first arise. Thus, mathematical models play an important role in understanding the problem. Several previous studies have investigated the contributions of pre-existence and/or production during treatment to the emergence of intra-host drug resistance, with varying degrees of theoretical development and quantification of specific scenarios. These have primarily dealt with HIV (Bonhoeffer and Nowak, 1997; Bonhoeffer et al., 1997; Ribeiro et al., 1998; Ribeiro and Bonhoeffer, 1999, 2000; Ribeiro, 1999; Roberts and Ribeiro, 2001; Gadhamsetty and Dixit, 2010; Shiri and Welte, 2011; Pennings, 2012), while the issue of pre-existing resistant variants has been analysed only to a limited extent in HCV models (Rong et al., 2010; Adiwijaya et al., 2010). Relatively few of these studies (Bonhoeffer and Nowak, 1997; Bonhoeffer et al., 1997; Ribeiro, 1999; Ribeiro and Bonhoeffer, 2000; Pennings, 2012) consider both pre-existence and production during treatment together. The most systematic theoretical comparison to date (Ribeiro and Bonhoeffer, 2000) concluded in the case of HIV that, over wide ranges of parameter space, pre-existence of resistant mutants is more likely than production after treatment begins. Exceptions occurred only when drug

* Corresponding author. Tel.: +41 44 6339252; fax: +41 44 6321271.
E-mail addresses: helen.alexander@env.ethz.ch (H.K. Alexander), sebastian.bonhoeffer@env.ethz.ch (S. Bonhoeffer).

1755-4365
http://dx.doi.org/10.1016/j.epidem.2012.10.001

efficacy was low or the cost of resistance was moderate to high (Ribeiro and Bonhoeffer, 2000).

Although questions regarding the source of resistance have primarily been addressed in the context of HIV, this issue is also relevant to other chronic viral pathogens, such as HBV and HCV. Although these viral infections share many similar features, there are also a number of qualitative and quantitative differences among the viruses' life cycles. For instance, the error-prone replication step giving rise to most mutations occurs in the production of virions for HBV and HCV, versus the integration of the provirus in HIV (Ganem and Schneider, 2001; Lindenbach and Rice, 2001; Mansky and Temin, 1995). Furthermore, infected cells are much longer-lived in HBV than in HIV (Nowak et al., 1996; Ribeiro et al., 2002; Soriano et al., 2008). We are therefore interested in determining whether the results obtained for HIV can be extended to viruses with different life cycles and drugs with different modes of action.

Despite differences in viral life cycles, models describing the dynamics of HIV, HBV and HCV have a similar structure (Nowak and May, 2000; Perelson, 2002; Ribeiro et al., 2002). It is thus a natural step to develop a single model that attempts to account for different viral life cycles in a more general framework. We focus on a stochastic model, capturing the effects of rare mutations and small population sizes. Earlier work on pre-existence and emergence was initially limited to deterministic models (Bonhoeffer and Nowak, 1997; Bonhoeffer et al., 1997; Ribeiro et al., 1998). Later stochastic models of the treatment phase did not analyse the role of stochastic loss of beneficial mutants (Ribeiro and Bonhoeffer, 2000; Roberts and Ribeiro, 2001), or investigated this factor only to a limited extent (Pennings, 2012). Here we develop robust analytical approximations for a stochastic model, which allow us to identify key parameter dependencies and readily explore parameter space, thus investigating the generality of our findings.

In the following section, we present a unified viral dynamics model. We then develop analytical approximations to the probability of resistance emerging from mutants arising before or after treatment begins. In this framework, we can explore the impact of various parameters as well as structural differences in life cycles, including the mechanisms of mutation, cost of resistance, and drug action. We investigate the situations in which mutants pre-existing and/or arising during treatment make a substantial contribution, and also consider the speed with which resistance rises during treatment. We conclude with a discussion of these findings in light of the differences among HIV, HCV, and HBV, as well as the more general problem of drug resistance in pathogens.

Model

We expand upon a model of intra-host viral dynamics which has been used widely in the literature, see e.g. Nowak and May (2000), Perelson (2002), including in previous studies of pre-existence and emergence in HIV (Bonhoeffer and Nowak, 1997; Bonhoeffer et al., 1997; Ribeiro et al., 1998; Ribeiro and Bonhoeffer, 1999, 2000; Ribeiro, 1999; Roberts and Ribeiro, 2001) and HCV (Rong et al., 2010; Adiwijaya et al., 2010). Besides facilitating comparison with much previous work, this population dynamics framework provides a convenient and natural representation to capture life cycle details. Nonetheless, alternative approaches could also be used to describe such a system; for instance, a few previous studies of drug resistance in HIV have modelled populations in discrete time steps with given fitness values (Gadhamsetty and Dixit, 2010; Pennings, 2012) and made use of results from population genetics (Pennings, 2012).

For two strains of virus, we model five populations: uninfected target cells (x), cells infected by the drug-sensitive (wild type) strain (y_S), cells infected by the drug-resistant (mutant) strain (y_R), drug-sensitive free virions (v_S) and drug-resistant free virions (v_R). We generalize from previous work to allow any virus-related parameters to be strain-specific, and for mutations to happen at either the cell infection step or the virion production step. We suppose that the drug(s) work by blocking these same steps. For completeness, we also include the loss of free virions during infection events. Then the ODE form of the model is:

$$\dot{x} = \lambda - dx - \beta_S(1-\epsilon_I)xv_S - \beta_R xv_R \tag{1a}$$

$$\dot{y_S} = \beta_S(1-\epsilon_I)(1-u_I)xv_S + \beta_R u_I xv_R - a_S y_S \tag{1b}$$

$$\dot{y_R} = \beta_S(1-\epsilon_I)u_I xv_S + \beta_R(1-u_I)xv_R - a_R y_R \tag{1c}$$

$$\dot{v_S} = -\beta_S xv_S + k_S(1-\epsilon_P)(1-u_P)y_S + k_R u_P y_R - c_S v_S \tag{1d}$$

$$\dot{v_R} = -\beta_R xv_R + k_S(1-\epsilon_P)u_P y_S + k_R(1-u_P)y_R - c_R v_R \tag{1e}$$

The parameters of this model are the target cell production rate, λ; the target cell natural death rate, d; the strain-specific infectivities, β_S and β_R; the infected cell death rates, a_S and a_R; the virion production rates, k_S and k_R; and the free virion clearance rates, c_S and c_R. For simplicity, we assume in the following that λ is a constant. More generally, λ can be taken as a function of (x, y_S, y_R), as has been done for example in hepatitis where the homeostatic proliferation of hepatocytes can be significant (Dahari et al., 2007; Guedj et al., 2010; Rong et al., 2010).

We model mutation according to a "stamping machine" mode of replication (Sanjuán et al., 2010; Loverdo et al., 2012), in which the mutation rates are u_I at the infection step and u_P at the virion production step. Depending on the life cycle of a particular virus, setting either $u_I = 0$ or $u_P = 0$ may be more appropriate. For instance, for a retrovirus such as HIV the major source of mutations is reverse transcription of viral RNA into proviral DNA, prior to integration into the host genome, by an error-prone viral enzyme (Goff, 2001; Mansky and Temin, 1995). This would be represented by $u_I > 0$, accounting for mutations in the formation of an infected cell, and $u_P \approx 0$ since transcription of RNA for progeny virions uses a host enzyme (Goff, 2001), which is of higher fidelity. Indeed, HIV-specific multi-strain models that explicitly include free virions, including Bonhoeffer et al. (1997), typically include mutation only at the cell infection step. On the other hand, for hepatitis C, the error-prone steps using viral polymerases occur in the production of individual progeny virions (Lindenbach and Rice, 2001). Although the life cycle includes in part binary (not only stamping machine) replication (Sanjuán et al., 2010), taking $u_P > 0$ and $u_I = 0$ in our framework seems a reasonable first approximation, which has been used previously in multi-strain HCV models (Rong et al., 2010; Adiwijaya et al., 2010; Guedj and Neumann, 2010).

By modelling only two strains of virus, we suppose that the overall mutation rate, $u \equiv u_I$ or u_P, is an effective rate accounting for whatever underlying genetic change confers drug resistance. For instance, if n site changes are required, taking $u = \tilde{u}^n$, where $\tilde{u}$ is the per-site mutation rate, is a good approximation if all intermediate strains have low fitness (which would typically be the case under combination drug treatment). If any of n single site changes from the wild type confer resistance, with all resistant strains having similar properties, then $u \approx n\tilde{u}$. More generally, an appropriate re-scaling of mutation rate should be able to capture the mean rate of mutational flow from wild type to fully resistant; however, we do not expect to capture higher moments. Details of the mutational pathway(s) to full resistance may indeed be important, but also add many parameters to the system. As a first approach, we thus make the approximation of two strains with an effective mutation rate.

Treatment is modelled by drug action at two possible steps of the replication cycle. A drug that blocks infection of target cells, such as an entry, reverse transcriptase or integrase inhibitor for

HIV, reduces the successful infection rate of the sensitive strain by a factor ϵ_I, called the efficacy. We assume that the free virion is always lost in an "attempted" infection, whether or not blocked by drug. A drug that blocks production of viable virions, such as a protease inhibitor for HIV or HCV, reduces the rate at which drug-sensitive infected cells produce (viable) virions by the efficacy ϵ_P. Some drugs, such as lamivudine for HBV, may exert effects at both steps (Nowak et al., 1996; Ribeiro et al., 2002). If a drug is not present, the corresponding efficacy is set to zero, while the maximal efficacy is one. We assume here that the resistant strain is fully resistant, and thus the factors of $(1-\epsilon)$ are applied only to the sensitive strain.

We quantify fitness of a strain by its basic reproductive number, R_0, in the corresponding single strain model. For an intra-host viral disease, R_0 can be defined as the expected number of new infected cells produced in one cycle of replication from a single infected cell introduced to an uninfected population (Nowak and May, 2000). The basic reproductive number of the sensitive strain in the absence of drug is thus $R_0^0 = (\lambda\beta_S k_S)/(d a_S c_S)$, if we neglect loss of free virions when infecting cells (this approximation is discussed below). In practice, we take drug efficacies under treatment sufficiently high such that $R_0^S = R_0^0(1-\epsilon_I)(1-\epsilon_P)$ is less than one. The resistant strain is assumed to have some cost of resistance, s, defined such that the basic reproductive number of the resistant strain is $R_0^R = R_0^0(1-s)$. We assume the same cost applies to the resistant strain whether or not drug is used. Previous multi-strain population dynamic models, e.g. Bonhoeffer and Nowak (1997), Ribeiro and Bonhoeffer (2000), Gadhamsetty and Dixit (2010), Rong et al. (2010), Adiwijaya et al. (2010), have typically assumed costs through one particular trait. This assumption may be realistic; for instance, there is biological evidence to suggest that the cost of protease inhibitor resistance in HCV should be borne by the virion production rate (Adiwijaya et al., 2010). Furthermore, for HIV, known drug resistance mutations typically occur in the drug target (Goldberg et al., 2012; Johnson et al., 2011), suggesting that the cost is also likely to be incurred through the function of the target protein. However, one could argue that general metabolic costs, as well as pleiotropic effects (e.g. a mutation in the HIV envelope gene making virions more visible to the immune system), could give rise to costs via other traits. Indeed, there is currently limited understanding of the exact mechanisms of fitness costs. Experimental fitness assays to date generally do not allow one to pinpoint the affected trait or measure genetic differences in more than one trait (Rong et al., 2007; Gadhamsetty and Dixit, 2010). This motivates us to consider a more general model where the resistant strain may differ in any viral trait (β, a, k, or c). For illustration in numerical results, we will take a cost in only one trait at a time, such that $\beta_R = (1-s)\beta_S$, $k_R = (1-s)k_S$, $a_R = a_S/(1-s)$, or $c_R = c_S/(1-s)$. However, the model and analysis still apply when the cost manifests itself through multiple traits, in which case the extent of the cost to each individual trait must be specified. In principle, s may take on any value between 0 and 1, and there is evidence that the cost of resistance indeed varies widely (see Supplementary Material). Here we show results under treatment with s chosen such that $R_0^R > 1$; otherwise, the resistant strain could not persist in the presence of drug.

For analytical approaches, the model can be simplified by making two assumptions that are widely used in the literature and can be justified for parameter estimates in diseases of interest; see Supplementary Material for details. Firstly, we assume that the loss rate of virions through infection is negligible relative to clearance, which is valid when the burst size (k/a) is considerably larger than the basic reproductive number (R_0^0). Secondly, we assume that the dynamics of free virions are much faster than those of infected cells, which is valid when virion production (k) and clearance (c) rates are large (Lloyd, 2001). We then have the quasi-equilibrium relationships:

$$v_S \approx \frac{k_S}{c_S}(1-\epsilon_P)(1-u_P)y_S + \frac{k_R}{c_S}u_P y_R$$
$$v_R \approx \frac{k_S}{c_R}(1-\epsilon_P)u_P y_S + \frac{k_R}{c_R}(1-u_P)y_R \quad (2)$$

and the following approximation of system 1:

$$\dot{x} = \lambda - dx - \left(\frac{\beta_S k_S}{c_S}(1-\epsilon_I)(1-\epsilon_P)(1-u_P) + \frac{\beta_R k_S}{c_R}(1-\epsilon_P)u_P\right) xy_S - \left(\frac{\beta_S k_R}{c_S}(1-\epsilon_I)u_P + \frac{\beta_R k_R}{c_R}(1-u_P)\right) xy_R \quad (3a)$$

$$\dot{y_S} = \left(\frac{\beta_S k_S}{c_S}(1-\epsilon_I)(1-\epsilon_P)(1-u_I)(1-u_P) + \frac{\beta_R k_S}{c_R}(1-\epsilon_P)u_I u_P\right) xy_S + \left(\frac{\beta_S k_R}{c_S}(1-\epsilon_I)(1-u_I)u_P + \frac{\beta_R k_R}{c_R}u_I(1-u_P)\right) xy_R - a_S y_S \quad (3b)$$

$$\dot{y_R} = \left(\frac{\beta_S k_S}{c_S}(1-\epsilon_I)(1-\epsilon_P)u_I(1-u_P) + \frac{\beta_R k_S}{c_R}(1-\epsilon_P)(1-u_I)u_P\right) xy_S + \left(\frac{\beta_S k_R}{c_S}(1-\epsilon_I)u_I u_P + \frac{\beta_R k_R}{c_R}(1-u_I)(1-u_P)\right) xy_R - a_R y_R \quad (3c)$$

In the majority of this manuscript we focus on the corresponding stochastic version of the model, which is a continuous-time Markov process with transition rates according to the rates of the ODE model. (Note however that the given system of ODEs does not exactly describe the means in this stochastic model, due to correlations between population sizes: see Heffernan and Wahl (2005).) We use the simplified system 3 to derive analytical approximations. Importantly, however, we conduct simulations of the full system 1, which provides a check that the results are robust to the model simplifications. Figures use a standard set of parameter values unless otherwise specified. Details of simulation methods and parameter values are provided in Supplementary Material.

Results

Life cycle effects on the mutation-selection balance

Before treatment begins, the resistant strain has a selective disadvantage relative to the sensitive strain, and is thus observed in a mutation-selection balance. In the deterministic model, the observed mutant frequency depends on features of the life cycle.

Taking $\epsilon_I = \epsilon_P = 0$ to represent the absence of drug, we can solve for the approximate pre-treatment infected equilibrium (x^*, y_S^*, y_R^*) in the simplified ODE model:

$$x^* = \frac{a_S c_S}{\beta_S k_S} = \frac{x_0}{R_0^0} \quad (4a)$$

$$y_S^* = \frac{\lambda}{a_S} - \frac{d c_S}{\beta_S k_S} \quad (4b)$$

$$y_R^* = \frac{(a_S/a_R)(u_I + (\beta_R c_S)/(\beta_S c_R)u_P)}{s} y_S^* \quad (4c)$$

where $x_0 = \lambda/d$ is the uninfected equilibrium level of target cells. (See Supplementary Material for derivation.) In particular, we can

consider the special cases where the cost manifests itself through a single trait:

$$\frac{y_R^*}{y_S^*} = \begin{cases} \dfrac{u_I + (1-s)u_P}{s}, & \text{for a cost through } \beta \text{ or } c \\ \dfrac{(1-s)(u_I+u_P)}{s}, & \text{for a cost through } a \\ \dfrac{u_I+u_P}{s}, & \text{for a cost through } k \end{cases} \tag{5}$$

Note that these expressions do not always coincide with the classical mutation-selection balance of u/s (with $u \equiv u_I + u_P$ the total mutation rate), although in all cases they do approach this ratio for small s. Rather, the frequencies depend on the life history trait through which the cost manifests itself and the step of the life cycle at which mutation acts, with strongest effect when the cost (s) is large. To gain an intuitive understanding, consider the limiting case of large cost ($s \to 1$, such that $R_0^R \to 0$). This means that a mutant is unable to complete a full life cycle. However, the observed frequency of mutants depends on the particular step(s) of the life cycle affected. We can distinguish between costs to persistence and costs to productivity. By "persistence", we mean any trait that affects the ability of a mutant to survive from de novo production through to and including the infected cell stage; that is, a in any case, and additionally β and c if the mutant first arises in virion production. By "productivity", we mean any trait that affects the rate at which a mutant infected cell generates new infected cells: that is, k in any case, and additionally β and c if the mutant first arises in cell infection. If a mutant is defective in persistence, in the limit it will die so quickly that it will never be present (as an infected cell). However, if a mutant is defective only in productivity, it will still be present at non-zero frequency, since it is continually generated by de novo mutation from the wild type and has no deficiency in survival once generated.

We also observe that the mutant frequency is not necessarily the same among free virions as it is among infected cells, although interchanging the corresponding parameters for mutation, production and loss rates gives parallel results (Supplementary Material). The effects of β and c are identical in our model framework, because these are parameters related to free virions, wrapped into one step by the quasi-equilibrium approximation. The grouping of parameter effects switches if we look at the frequency among free virions (Supplementary Material). If $u_P = 0$ (resp. $u_I = 0$), the differences among parameters further collapse, since there is no possibility of a mutant first arising in the free virion (resp. infected cell) stage.

Distribution of mutant population size

In the pre-treatment phase, a mutant strain with a cost will be rare, maintained only by continual mutation from the wild type, and thus subject to significant stochasticity. The population size is not well captured by its average or deterministic prediction alone, but can be better described through its entire probabilistic distribution. At "equilibrium", i.e. once the population size distributions have stabilized, this distribution can be well approximated by the steady state of a birth-death-immigration (BDI) process with constant parameters.

Specifically, the mutant population (y_R) follows a BDI process where "birth" represents replication of a mutant infected cell, by generating infection in another target cell; "death" is death of a mutant infected cell; and "immigration" represents de novo mutation from the wild type. The key to this approximation is to suppose that target cells and wild type infected cells (x and y_S, respectively) are effectively at their deterministic equilibrium population sizes, yielding constant rates for each of the aforementioned events. Although the populations do show stochastic fluctuations, these variations are small relative to the means, and have minimal effect on the mutant infected cell population.

In Supplementary Material, we identify the rates of these events and apply standard results (Kendall, 1949) to obtain the following probability generating function (PGF) for the distribution of mutant population size at the pre-treatment equilibrium:

$$\psi(z) = \left(\frac{s}{1-(1-s)z}\right)^{(a_S/(a_R(1-s)))(u_I+(\beta_R c_S)/(\beta_S c_R)u_P)y_S^*} \tag{6}$$

(The variable z here is a placeholder in the generating function, see e.g. Wilf (1994); it is not associated with a particular quantity in the model.) The function is particularly simple for costs through single traits:

$$\psi(z) = \begin{cases} \left(\dfrac{s}{1-(1-s)z}\right)^{(u_I/(1-s)+u_P)y_S^*}, & \text{for a cost through } \beta \text{ or } c \\ \left(\dfrac{s}{1-(1-s)z}\right)^{(u_I+u_P)y_S^*}, & \text{for a cost through } a \\ \left(\dfrac{s}{1-(1-s)z}\right)^{((u_I+u_P)/(1-s))y_S^*}, & \text{for a cost through } k \end{cases} \tag{7}$$

Hence the distribution of the number of pre-existing mutants depends on the wild type infected cell population size, as well as the probability of mutation and the cost of the mutation at each step of the life cycle. It does not, however, depend on the precise parameter values associated with the virus, so long as we know the costs relative to the wild type.

In a more specialized model, the same approach has previously been used to approximate the distribution of mutant population size at equilibrium (Ribeiro, 1999). However, the method was used only to find the probability of having zero mutants, the mean and the variance of the distribution. Here we investigate the entire distribution, as well as generalizing to various viral life cycles.

The analytical approximation generally shows an excellent fit to simulation results: see Fig. 1. The left column shows costs through β; the right column, through a. Substantial differences arise only when s is sufficiently large. Specifically, when comparing two costly traits with a given mutational step, the proportional reduction in the mean number of mutants is either 0 or s (see Eq. (5)). Correspondingly, life cycle differences have only a small effect on the entire distribution when s is small (top row). However, when s is larger, the distributions may differ substantially, as illustrated in the middle and bottom rows. Comparing left to right panels, we see how cost via different traits can affect the number of mutants present, while comparing middle to bottom panels, we see the impact of mutation mechanism. Depending on the costly trait, the step at which mutations occur may or may not affect the distribution, and vice versa. Overall, these results show the potentially large effect of life cycle when costs are not small, while highlighting the point that it is the interaction between mutational step and costly step that matters.

As $s \to 0$, all parameters collapse to the wild-type values. However, it is not surprising that the dependence on the particular mechanism of the cost increases with the magnitude of the cost. We can consider the limiting case analytically by taking the limit as $s \to 1$ in the PGF (Eq. (6)). It turns out that for any single-trait cost, the limiting distribution is Poisson, with mean given by the deterministic y_R^* evaluated at $s = 1$. Thus, the results agree with the intuition developed in Section "Life cycle effects on the mutation-selection balance": in particular, for mutants defective in persistence, the distribution approaches a point mass at zero, while for mutants defective in productivity, the distribution has a non-zero mean. In a stochastic setting, we can understand the form of the limiting distribution by noting that if a mutant cannot complete its replication cycle, every mutant present must be generated de novo from the wild type. These events occur according to a pure

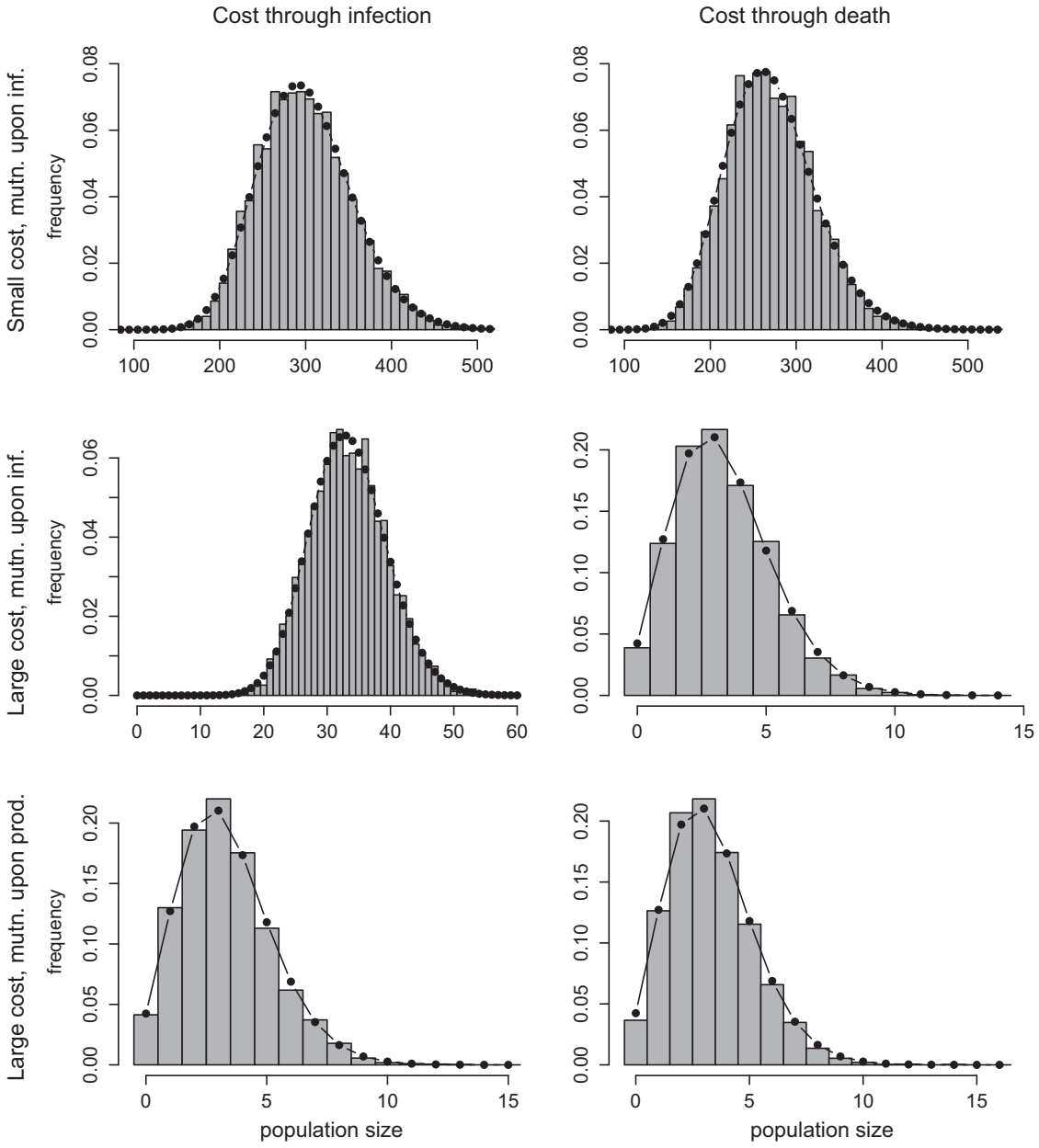

Fig. 1. The distribution of the number of mutant infected cells (y_R) at pre-treatment equilibrium, for various life cycles and costs. Grey bars show the frequency (probability) of a given population size among 5000 simulations, and points show the BDI approximation of the probability. Top two rows: mutation upon infection ($u_I > 0$); bottom row: mutation upon virion production ($u_P > 0$). Left column: cost through β; right column: cost through a. Costs are $s = 0.1$ (top row) or $s = 0.9$ (bottom two rows). In the top row, results are grouped by 10's for easier visualization; the vertical axis then shows the total probability of being within this range.

Poisson process with immigration rate I, and the mean number of mutant infected cells present is then given by the immigration rate times the average lifespan of a mutant infected cell ($I \times 1/a_R$). In general, for $s < 1$, the distribution of mutant population size is not simply Poisson, since de novo mutation (immigration) events are compounded by mutant self-replication. Nonetheless, it is possible through the BDI steady state to capture the full distribution analytically with high accuracy.

Target cell rebound and stochastic extinctions during treatment

Although the mutant strain is assumed to have fitness $R_0^R > 1$, and likely a substantial fitness advantage over the wild type during treatment, there is no guarantee that it will escape stochastic extinction when initially rare. That is, the persistence of mutants – not only their appearance – is a potentially significant component in evaluating risks, but one that has previously been considered only to a limited extent (Ribeiro, 1999; Ribeiro and Bonhoeffer, 2000; Roberts and Ribeiro, 2001; Pennings, 2012).

The chance that a mutant persists critically depends on the availability of target cells for new infections. When treatment begins, target cells are at the equilibrium set by the previously dominant wild type; under the assumption that the mutant carries a cost, this level is necessarily too low to support self-sustained growth of the mutant population. However, once a (sufficiently effective) drug blocks wild type infections, the target cell population gradually rebounds from pre-treatment levels towards the uninfected equilibrium, conferring an ever-increasing infection rate on the mutant

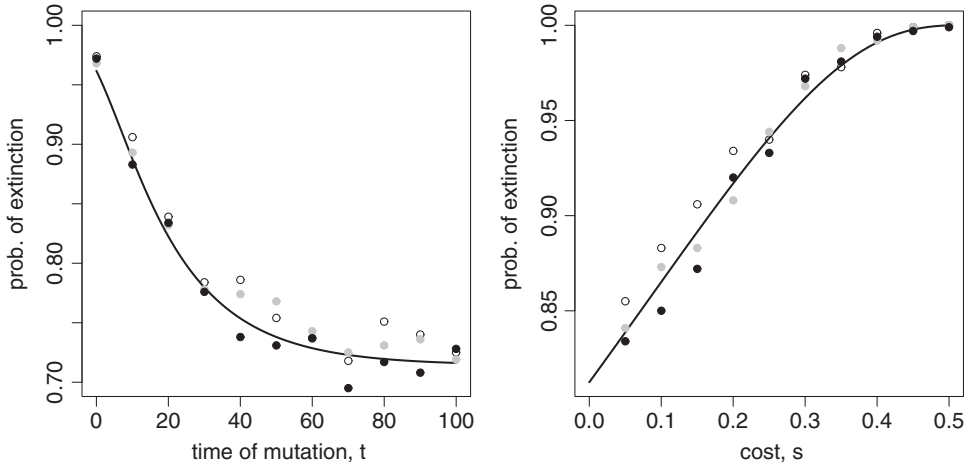

Fig. 2. The probability of extinction of a single mutant's lineage during the treatment phase. The solid line shows the analytical approximation given by Eq. (8) and the points show simulation results with various drug efficacies (black: $\epsilon = 1$, grey: $\epsilon = 0.8$, unfilled: $\epsilon = 0.55$). Drug is assumed to act by blocking cell infection ($\epsilon_I \equiv \epsilon$; $\epsilon_P = 0$) and the cost of resistance is taken through infectivity (β). Left: A single mutant is introduced at time t after treatment starts, with a cost of $s = 0.3$. Right: A single mutant exists at the time treatment starts ($t = 0$) and probability of extinction is plotted as a function of cost, s.

population. This implies that mutants arising later are predicted to have a better chance at escaping extinction, and in particular, any mutant that arises before the target cell population has rebounded to the infected equilibrium level set by the mutant strain must persist until this point in order to have a non-zero chance at escaping extinction.

We have derived an analytical approximation for the probability that a single mutant existing at a given time after treatment initiation escapes early stochastic extinction and thus has long-term descendants. Details can be found in Supplementary Material. Briefly, we model the population descending from one progenitor with a time-inhomogeneous birth-death process. Births (i.e. new infections) and deaths occur very similarly to the pre-treatment phase; the key difference is that the target cell population (and hence the birth rate) is now time-dependent. We find that a mutant existing at time t after treatment starts ultimately has no surviving descendants with probability:

$$p_{\text{ext}}(t) = 1 - (1 + \gamma_R \exp(g_1(\gamma_R e^{-dt}, R_0^0, s))(g_1(\gamma_R e^{-dt}, R_0^0, s))^{-g_2(\gamma_R, R_0^0, s)} \cdot \Gamma(g_2(\gamma_R, R_0^0, s), 0, g_1(\gamma_R e^{-dt}, R_0^0, s)))^{-1} \quad (8)$$

where $\gamma_R = a_R/d$ represents the relative infected cell death rate (as per the definition in (Ribeiro, 1999; Ribeiro and Bonhoeffer, 2000)), and we define for convenience the functions $g_1(\gamma, R_0, \xi) = \gamma(R_0 - 1)(1 - \xi)$ and $g_2(\gamma, R_0, \xi) = \gamma(R_0(1 - \xi) - 1)$. Furthermore, $\Gamma(z, c_1, c_2) := \int_{c_1}^{c_2} x^{z-1} e^{-x} dx$ is the generalized incomplete gamma function.

Importantly, this probability is a function of the time at which the mutant arises. This time is scaled relative to the uninfected cell death rate, d, which defines the rate at which target cells rebound. Since target cell availability is increasing, the total birth rate is also increasing and hence the chance of extinction is decreasing over time, as illustrated in Fig. 2 (left). Eq. (8) shows that the probability of extinction depends on three further key parameters: the selective disadvantage, s; the death rate of mutant infected cells, relative to uninfected cells, γ_R; and the baseline reproductive number, R_0^0. As expected, the probability of extinction increases with s, as shown in Fig. 2 (right). The intuition that the probability of extinction increases with infected cell death rate is also supported numerically. This means that a mutant with a cost through higher death rate (a) will always have a smaller chance of escaping extinction than a mutant with the same fitness cost but through lower "birth" rate (i.e. through any parameter affecting the rate at which infected cells are generated: β, k, or c). Finally, it can be shown that the "birth" rate of infected cells is increasing with the baseline reproductive number R_0^0, and hence the probability of extinction decreases with R_0^0. That is, the increased per-target-cell replicative capacity outweighs the greater pre-treatment depletion of target cells. The drug efficacy ϵ does not appear in the analytical expression for the probability of extinction, since we assume that target cells rebound as if no further infections occur. However, we expect the approximation to be an underestimate of extinction for lower values of ϵ, since a drug that allows more ongoing replication of the wild type will lead to more competition for target cells than predicted. Nonetheless, simulation results using various drug efficacies (points in Fig. 2) show that the approximation (solid line) is fairly robust to this assumption.

Contributions of pre-existence and rescue

As described in the Introduction, there has been considerable interest in comparing the contributions to the emergence of resistance made by "pre-existing" versus "rescue" mutants. The term pre-existence is used widely in the literature, e.g. Bonhoeffer and Nowak (1997), Ribeiro and Bonhoeffer (2000), Rong et al. (2010), and refers to mutants arising de novo before treatment begins and present when treatment starts. Rescue mutants are defined here as mutants that are generated de novo after treatment starts and that have long-term descendants. The term rescue is borrowed from the conservation biology and population genetics literature (Orr and Unckless, 2008; Bell and Gonzalez, 2009) and there refers to the outgrowth of any mutant, while here we reserve the term only for mutants that arise during the treatment phase.

Our general approach to calculating the probability of emergence of resistance (i.e. viral population survival under treatment) is first to consider how mutants arise, thus determining the number and timing of incipient lineages. The viral population fails to persist if and only if all these lineages die out; we can approximate this probability by treating each lineage independently. We apply this approach separately to mutants arising either before or after treatment initiation, in order to isolate each contribution.

Pre-existence

Assuming treatment begins after the system has equilibrated, the total number of pre-existing mutants, N, has a distribution approximated by the birth-death-immigration steady state

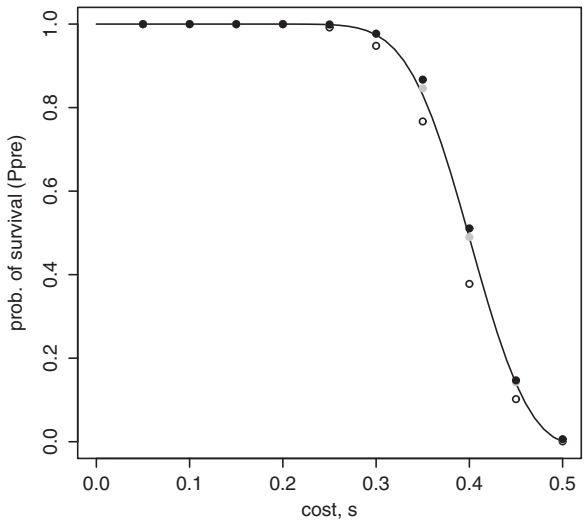

Fig. 3. The total probability of survival due to pre-existing mutants, as a function of the cost of resistance s (incurred through infectivity β here, with mutations at the cell infection step). The solid line shows the analytical approximation given by Eq. (9) and the points show the proportion of simulations (1000 per point) surviving to the end of the run (various drug efficacies – black: $\epsilon_I = 1$, grey: $\epsilon_I = 0.8$; unfilled: $\epsilon_I = 0.55$; all with $\epsilon_P = 0$).

distribution, with PGF $\psi(z)$ given by Eq. (6). Thus, the probability of survival due to pre-existence, under independence, is:

$$P_{\text{pre}} = 1 - \sum_{n=0}^{\infty} Pr(N = n) p_{\text{ext}}(0)^n = 1 - \psi(p_{\text{ext}}(0)) \tag{9}$$

This probability depends on two components: the number of mutants pre-existing (investigated in Section "Distribution of mutant population size") and each one's chance of survival once treatment starts (Section "Target cell rebound and stochastic extinctions during treatment"). The first component is affected by cost of resistance, mutation probabilities, and pre-treatment wild type infected cell population size; and the second component, by relative infected cell death rate, baseline reproductive number, and again cost.

Fig. 3 illustrates the dual disadvantage incurred by the cost of resistance: (1) there are fewer mutants to begin with and (2) each mutant is less likely to survive, due to inefficient replication, which requires a greater extent of target cell rebound to sustain growth. Thus, as s increases, the probability of survival drops off sharply. The analytical approximation again shows very good agreement to simulation results and robustness to varying drug efficacy.

Rescue

We model the appearance of rescue mutants with a time-inhomogeneous Poisson process. The rate at which mutants arise during treatment depends on the level of residual replication of the wild type and the probability of mutation. The total rate of de novo mutation thus declines with the wild type population over time. Furthermore, a mutant is only counted as a rescue mutant if its lineage ultimately escapes extinction. Thus the rate of appearance is weighted by the time-dependent probability of escaping extinction considered in Section "Target cell rebound and stochastic extinctions during treatment". These factors together give the rate of events in the Poisson process over time. Applying results for time-inhomogeneous Poisson processes (Parzen, 1999), we have the following expression for the probability that rescue occurs:

$$P_{\text{resc}} = 1 - \mathrm{e}^{-\int_0^\infty (1/d)\nu(t/d)dt} \tag{10}$$

where $\nu(t)$ is the rate of appearance of rescue mutants (i.e. those that ultimately have surviving descendants) at time t after treatment begins:

$$\nu(t) = dy_S^* R_0^0 \gamma_S (1-\epsilon_P)\left((1-\epsilon_I)u_I + \frac{\beta_R c_S}{\beta_S c_R} u_P\right)(1-(1-1/R_0^0)\mathrm{e}^{-dt}) \times \exp(g_1(\gamma_S, R_0^0, \epsilon)(\mathrm{e}^{-dt}-1) + g_2(\gamma_S, R_0^0, \epsilon)dt)(1-p_{\text{ext}}(t)) \tag{11}$$

(for derivation see Supplementary Material). Here $\epsilon := 1-(1-\epsilon_P)(1-\epsilon_I)$, $\gamma_S := a_S/d$, and the functions g_1 and g_2 are defined as for Eq. (8).

The total contribution of rescue mutation depends on the combined effects of the de novo mutant production rate and the chance that each mutant survives. The impacts of drug efficacies and mutation rates come in only through production; in particular, P_{resc} can be made arbitrarily low by taking sufficiently low mutation rate or, for certain life cycle and drug combinations (see below), sufficiently high drug efficacy. Note that the expression here for the rate of mutant appearance is not always independent of the cost of resistance; this is because we track the appearance of infected cells, and mutants that arise at the virion production stage must first avoid clearance and infect a target cell in order to be counted. Thus the "conversion factor" $\beta_R c_S/\beta_S c_R$ appears for mutants arising at the virion stage (via u_P). However, in a biological sense, properties of the mutant itself, including cost s and relative resistant infected cell death rate γ_R, only affect its survival and not its appearance. Uninfected cell death rate, d, does not affect P_{resc} separately from its contributions to R_0^0 and the relative infected cell death rates. Mathematically, this is because d only appears in the product dt, and we integrate over all time to obtain the probability of *eventual* extinction. Thus, d gives an intrinsic rescaling of time, affecting the speed of the dynamics but not the eventual outcome.

The quasi-equilibrium proportionality between free virus and infected cells is reached only after a full replication cycle under treatment. This necessitates a small correction to P_{resc} accounting for the contribution of new infections by pre-existing sensitive free virions. Adding the resistant infected cells produced by these sensitive virions yields the modified approximation:

$$P'_{\text{resc}} = 1 - \mathrm{e}^{-m_1(1-p_{\text{ext}}(0)) - \int_0^\infty (1/d)\nu(t/d)dt} \tag{12}$$

where m_1, the approximate expected number of mutant infected cells produced in the first cycle, is given by

$$m_1 = \frac{(1-\epsilon_I)u_I y_S^*}{c_S/a_S}$$

(see Supplementary Material for details).

Fig. 4 illustrates the dependence of the probability of rescue on cost of resistance and drug efficacy. We here use an HIV-like life cycle (mutations and cost at cell infection) with either a reverse transcriptase inhibitor or a protease inhibitor (drug acting at cell infection or virion production, respectively). The results are compared to three analytical approximations: our P_{resc} and P'_{resc} derived above, and the probability of producing at least one de novo mutant during treatment (excluding the first cycle of infection by free virions), without taking into account stochastic extinctions. The latter approximation is comparable to that used in some previous studies (Ribeiro, 1999; Ribeiro and Bonhoeffer, 2000). Simulation results generally align best with P'_{resc}, although the deviation from P_{resc} may be small. The probability of producing a mutant is independent of its cost s (for this life cycle). However, a mutant with a higher cost of resistance is less likely to escape extinction, such that the probability of survival declines with s, as shown in the top two rows. Thus, failing to account for stochastic extinctions yields the largest inaccuracies when the cost of resistance is high. On the other hand, to a good approximation, the drug efficacy plays no role in the

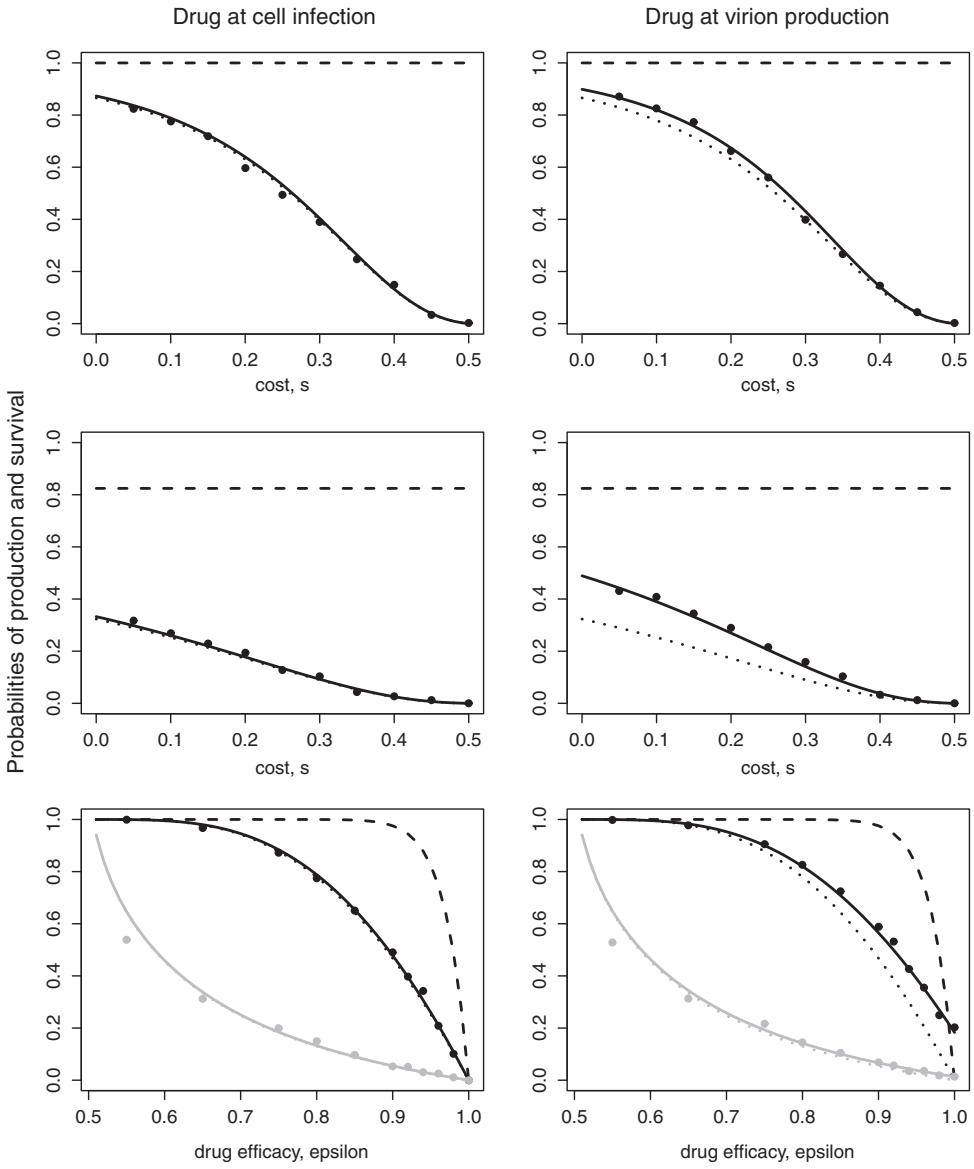

Fig. 4. The total probability of survival due to rescue mutation. The lines show analytical approximations – solid: P'_{resc} given by Eq. (12); dotted: P_{resc} given by Eq. (10) (excluding the first cycle of infections by free virions); dashed: probability of producing a mutant (excluding the first cycle and ignoring the chance of extinction). The points show simulation results (1000 runs per point). In all cases, we use a life cycle with mutation at cell infection ($u_I > 0$, $u_P = 0$) and a cost via infectivity (β). On the left, the drug blocks cell infection ($\epsilon_I \equiv \epsilon$); on the right, the drug blocks virion production ($\epsilon_P \equiv \epsilon$). Top row: probabilities as a function of cost of resistance s, for drug efficacy $\epsilon = 0.8$. Middle row: probabilities as a function of s, for $\epsilon = 0.95$. Bottom row: probabilities as a function of ϵ, for $s = 0.1$ (black) or $s = 0.4$ (grey).

persistence of a resistant mutant once produced. However, the higher the efficacy, the less residual replication of the sensitive strain, and thus the fewer de novo mutations occur. Therefore, both the probability of production and the total probability of survival decline with ϵ (bottom row).

Life cycle effects on pre-existence and rescue

A key point of interest is to investigate the impact of life cycle on the emergence of drug resistance. To this end, we consider the four life cycles illustrated in Fig. 5, taking each possible combination of mutation step and drug action step in our model framework. That is, we assume mutation occurs with probability u at either cell infection ($u_I \equiv u$) or virion production ($u_P \equiv u$), and that the drug acts with efficacy ϵ at either cell infection ($\epsilon_I \equiv \epsilon$) or virion production ($\epsilon_P \equiv \epsilon$). Of course, mutation or drug action could also occur at both steps, but we can view these four cases as the extremes. We suppose a cost may arise at any single step of the life cycle. At first, this appears to give rise to an inconveniently large number of possibilities to consider. However, through our analytical understanding of the probability of emergence, it turns out that the number of distinct cases collapses considerably.

First consider P_{pre}, which depends on the number of pre-existing mutants (captured by $\psi(z)$) and each one's chance of stochastic extinction (captured by $p_{\text{ext}}(0)$). The distribution of pre-existing population size depends on mechanisms of cost and mutation, but not on the drug. This distribution separates into two distinct cases: (1) when mutation occurs at cell infection and cost is via β, c, or k, or mutation occurs at virion production and cost is via k and (2) when mutation occurs at cell infection and cost is via a, or mutation occurs at virion production and cost is via β, c, or a. In particular, the mean of the distribution is higher in the first case. The chance of extinction depends on neither mechanism of mutation nor drug, but does depend on the mechanism of cost. Recall, however, that $p_{\text{ext}}(t)$ is identical for β, c, or k costs, and higher for a cost via a. In summary, we see that P_{pre} collapses into three cases, as illustrated

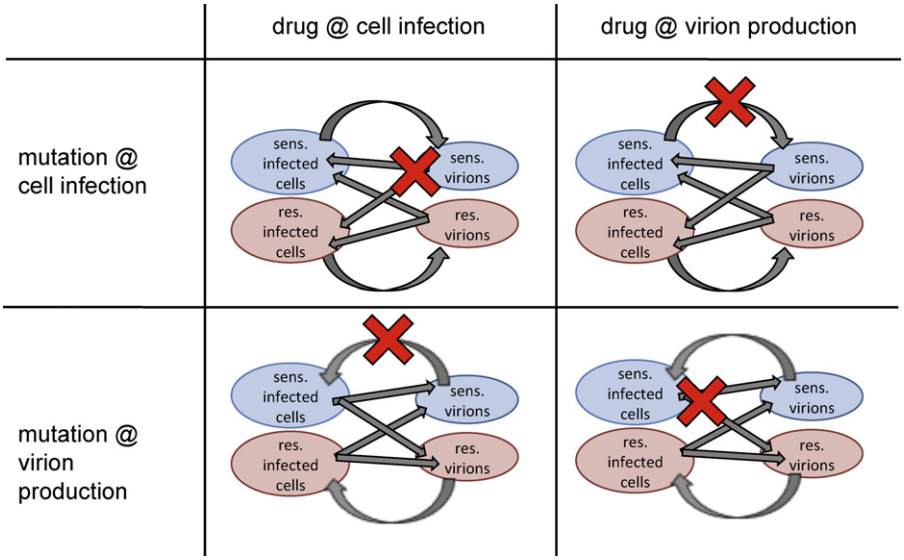

Fig. 5. Schematic diagram of the four life cycles under consideration. Arrows indicate production, and crosses indicate inhibition of this production by the drug.

in Supplementary Fig. 1. Note that, in the case of mutation at cell infection, increased infected cell death confers the dual disadvantage of a smaller pre-existing population size and a lower chance of escaping stochastic extinction.

Next we consider P'_{resc}, which can be characterized by the rate of rescue mutations, $\nu(t)$, and the expected number of "first round" mutants, m_1. We can write

$$\nu(t) = C(t)(1-\epsilon_P)\left((1-\epsilon_I)u_I + \frac{\beta_R c_S}{\beta_S c_R}u_P\right)(1-p_{\text{ext}}(t))$$

where the factor $C(t) := dy_S^* R_0^0 \gamma_S (1-(1-1/R_0^0)e^{-dt})\exp((e^{-dt}-1)g_1(\gamma_S, R_0^0, \epsilon) + g_2(\gamma_S, R_0^0, \epsilon)dt)$, declining over time with the wild type population, does not vary according to life cycle. Similarly, $m_1 = A(1-\epsilon_I)u_I$ where $A := y_S^*/(c_S/a_S)$ is independent of life cycle. Thus, the components of P'_{resc} in the various life cycles can be summarized as in Table 1.

Consider first the interaction between the mechanisms of mutation and cost. If mutation occurs at cell infection, any cost mechanism affecting the production rate of new infected cells (β, c, or k) is equivalent, while a cost affecting the loss rate of infected cells (a) yields a lower probability of survival. If mutation occurs at virion production, the situation is more complicated. Mutants first appear at the free virion stage, so a cost via c or β will reduce the chance that a mutant infected cell is subsequently produced. On the other hand, a cost via a will reduce the chance that a mutant infected cell has long-term descendants. Thus, P'_{resc} is highest if the cost is incurred via k.

Next we consider the interaction between the mechanisms of mutation and drug action. We refer to scenarios where the drug blocks the step at which mutation occurs as "synchronous". In these cases, a perfectly effective drug with $\epsilon = 1$ leads to $P'_{\text{resc}} = 0$, since there is no possibility to generate de novo mutants. On the other hand, if the drug effect and mutation step are "asynchronous", the drug is not directly blocking the generation of resistant mutants. In these cases, $\epsilon = 1$ does not lead to $P'_{\text{resc}} = 0$ because the pre-existing sensitive populations can still generate resistant mutants in the replication step uninhibited by drug. The difference between these two scenarios is most apparent when drug efficacy is high. A particularly high probability of rescue arises when mutations occur upon virion production and the drug blocks cell infection, since mutants are directly generated by relatively long-lived infected cells rather than short-lived free virions. Supplementary Fig. 2 illustrates the possible distinct cases.

When is rescue important?

We now have substantial analytical understanding of P_{pre} and P'_{resc} individually; however, it is not obvious how these quantities compare. Having demonstrated the accuracy of our approximations for these probabilities (preceding sections and Supplementary Material), we now investigate parameter effects using only analytical results. Since the question of which source contributes more to the emergence of resistance has been the topic of earlier studies, it is useful to delineate exactly how our work differs, particularly from previous work on an intra-host viral dynamics model taken in the single-locus case (Ribeiro and Bonhoeffer, 2000). To this end, there are two key differences in the model itself: we generalize across life cycles, and we take into account stochastic extinctions of rare mutants during the treatment phase. Moreover, there is a question of how to measure contributions of pre-existence and rescue.

Relative contributions have previously been quantified using expected numbers of mutants from each phase: specifically, the ratio $\mathbb{E}[\#\text{ mutants during treatment}]/\mathbb{E}[\#\text{ pre-ex. mutants}]$,

Table 1
Summary of rescue rates in the various life cycles. The factors $C(t)$ and A, defined in the main text, do not depend on life cycle.

	Drug at cell inf.	Drug at virion prod.
Mut. at cell inf., Any cost mech.	$\nu(t) = C(t)(1-\epsilon)u(1-p_{\text{ext}}(t))$ $m_1 = A(1-\epsilon)u$	$\nu(t) = C(t)(1-\epsilon)u(1-p_{\text{ext}}(t))$ $m_1 = Au$
Mut. at virion prod., k or a cost	$\nu(t) = C(t)u(1-p_{\text{ext}}(t))$ $m_1 = 0$	$\nu(t) = C(t)(1-\epsilon)u(1-p_{\text{ext}}(t))$ $m_1 = 0$
Mut. at virion prod., β or c cost	$\nu(t) = C(t)(1-s)u(1-p_{\text{ext}}(t))$ $m_1 = 0$	$\nu(t) = C(t)(1-s)(1-\epsilon)u(1-p_{\text{ext}}(t))$ $m_1 = 0$

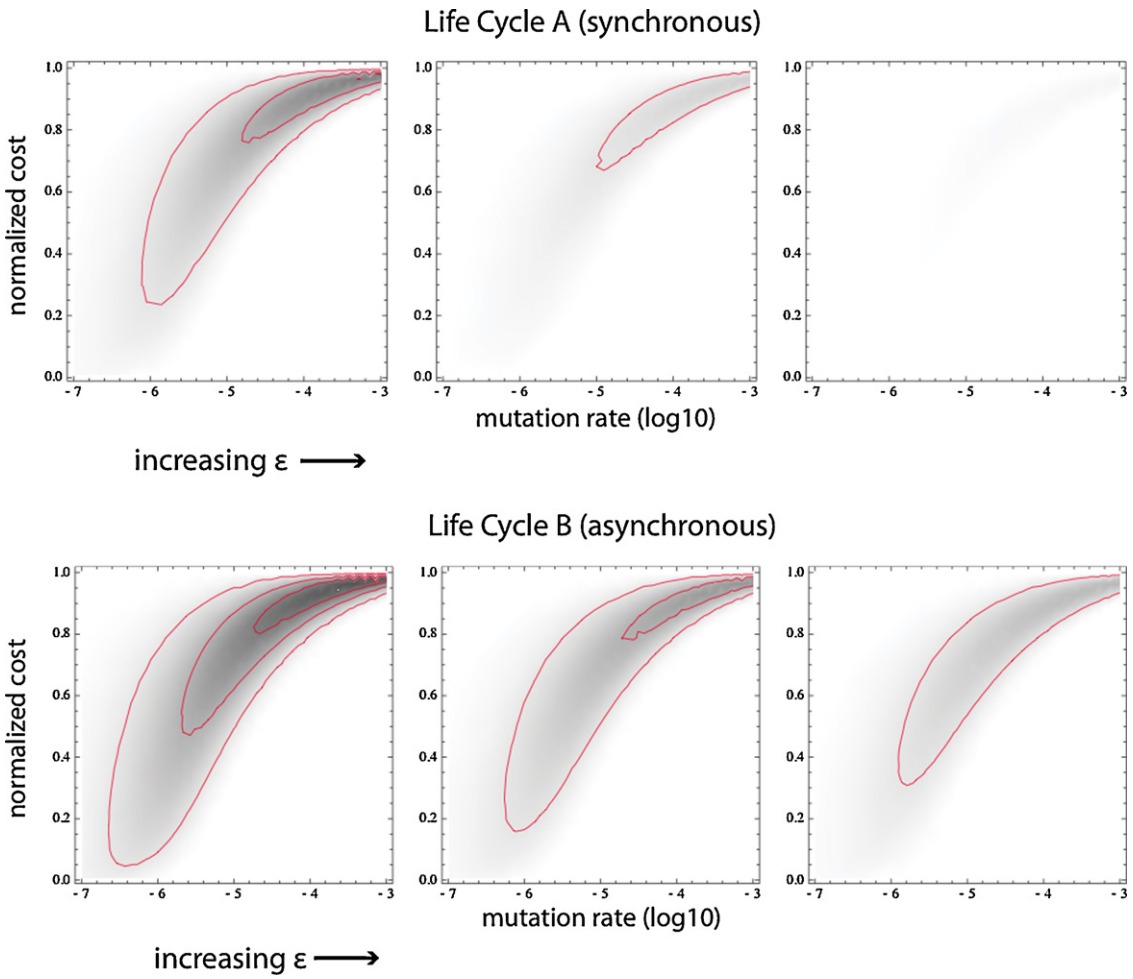

Fig. 6. Effect of drug efficacy ϵ on the relative importance of rescue, as measured by $P_{R\backslash P}$. Darker shading on the density plots corresponds to a larger value of $P_{R\backslash P}$ (white = 0, black = 1), and contour lines (red) indicate values of 0.1–0.9 in increments of 0.2. Top panels: Life Cycle A; bottom panels: Life Cycle B. The parameters $R_0^0 = 2$ and $\gamma = 10$ are fixed at their standard values, while u and s vary as indicated on the axes. s is normalized as a proportion of the maximum cost allowed, $s_{\max} = 1 - 1/R_0^0$. We select values of $\epsilon = 0.55$, 0.7 and 0.9, from left to right panels. (For interpretation of the references to colour in this figure legend, the reader is referred to the web version of the article.)

denoted Θ_1 (Ribeiro and Bonhoeffer, 2000). For direct comparison, we can define the corresponding ratio $\tilde{\Theta}_1$, which is valid for more general life cycles but otherwise differs only by taking stochastic extinction into account and by the (typically small) correction made for first-round replication of free virions (m_1). An analytical expression for $\tilde{\Theta}_1$, which elucidates parameter dependencies, is provided in Supplementary Material. First, $\tilde{\Theta}_1$ depends on the life cycle-specific parameters s, ϵ, and u. Second, it depends on the composite parameters γ_S, R_0^0 and c_S/a_S (which affects only the correction factor m_1). The population size y_S^* cancels out. Furthermore, if mutation occurs in only one step ($u_P = 0$ or $u_I = 0$), the non-zero mutation rate also cancels, as found previously for a particular life cycle (Ribeiro and Bonhoeffer, 2000). We also find that taking survival of mutant lineages into account always increases this measure of the relative contribution of mutants arising after treatment begins (see Supplementary Material). Intuitively, this is because mutants arising de novo during treatment encounter a higher level of target cells and thus a lower probability of extinction.

Although the above analysis is useful for direct comparison with previous work, we argue that a more relevant measure of contributions is the probability of having at least one survivor, rather than the expected number of survivors. The long-term outcome under treatment is the same regardless of how many founders of resistant lineages there are, so long as there is at least one. Furthermore, since pre-existence chronologically occurs first, we re-frame the question of relative contributions to ask, "When does rescue make an important contribution to the emergence of resistance?" That is, if pre-existence is virtually guaranteed to result in emergence, we have little interest in how many more rescue mutations subsequently occur. However in any case, for rescue to be significant, its probability must be sufficiently high. We therefore use the measure:

$$P_{R\backslash P} := (1 - P_{\text{pre}})P'_{\text{resc}}$$

which is, to a good approximation, the probability that no pre-existing mutants survive but at least one rescue mutant survives. This measure reflects when rescue is important in changing the outcome of a treated infection.

The measure $P_{R\backslash P}$ depends on the life cycle-specific parameters s, ϵ and $u \cdot y_S^*$ and the composite parameters γ_S, R_0^0 and c_S/a_S. In contrast to $\tilde{\Theta}_1$, the parameters y_S^* and u_I or u_P no longer cancel out, but only ever appear as products ($u_I y_S^*$ and $u_P y_S^*$) representing the total mutational influx. This is not surprising, since the population of sensitive infected cells is homogeneous and thus it does not matter from which particular cell a de novo mutant arises.

Since c_S/a_S typically has a minor effect (only via m_1), we focus on the effects of s, ϵ, γ_S, R_0^0, and u (with the understanding that y_S^* has an equivalent effect). For illustration, we select two life cycles,

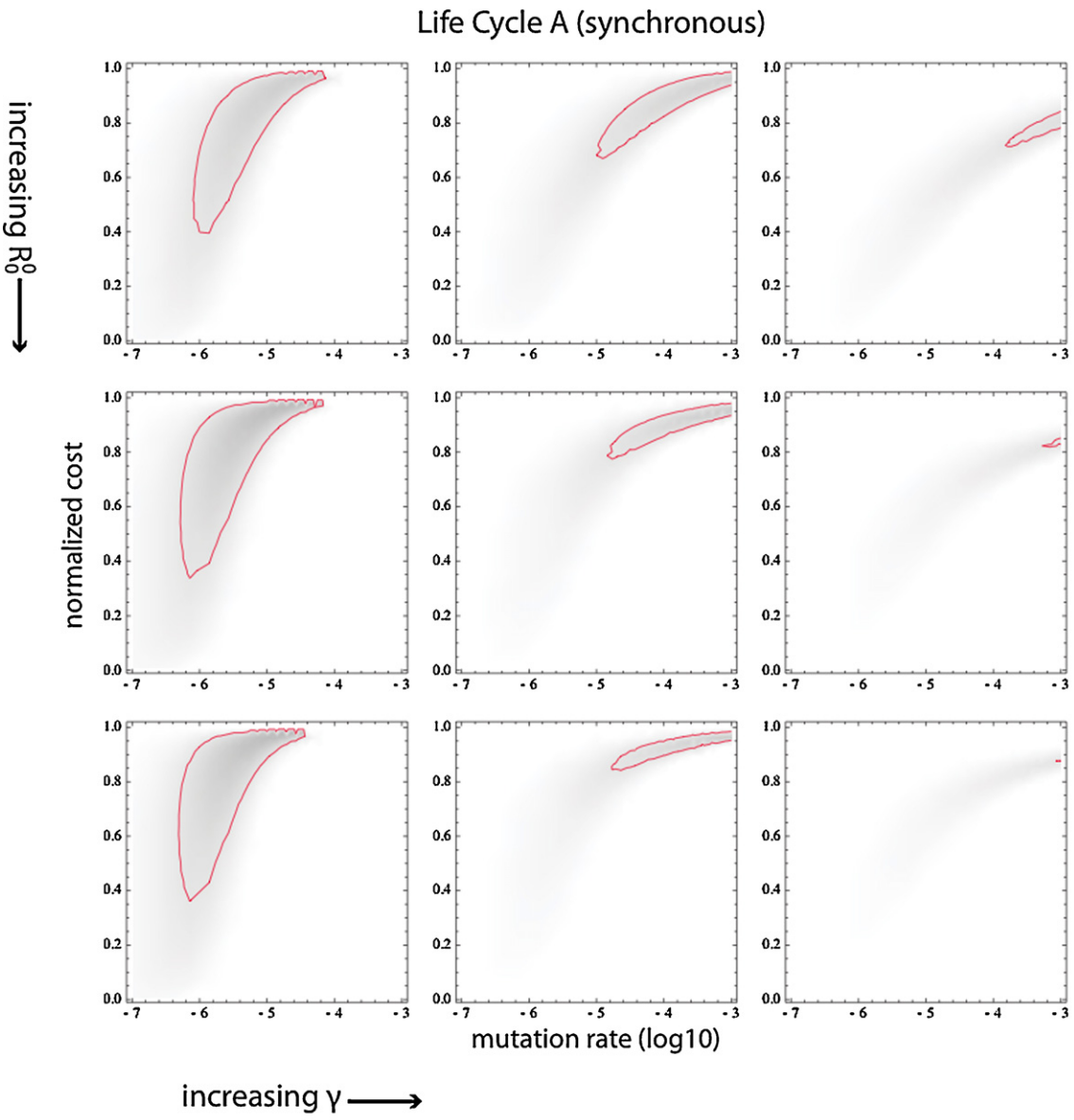

Fig. 7. Parameter effects on the relative importance of rescue, as measured by $P_{R\backslash P}$, in Life Cycle A. Shading and contours are the same as in Fig. 6. Drug efficacy ϵ is fixed for each R_0^0 such that R_0^S under treatment is an intermediate value of 0.6, while mutation rate u and cost s vary as indicated on the axes. s is normalized as a proportion of the maximum possible cost, $s_{max} = 1 - 1/R_0^0$, allowed for a given R_0^0. Relative infected cell death rate γ varies across each row over values (left to right) 2, 10, and 25. R_0^0 varies down each column over values (top to bottom) 2, 6, and 10.

which we found in the previous section to have highly divergent behaviour in P'_{resc}. Both have mutation at virion production and a cost through k, but Life Cycle A (synchronous) has the drug acting at virion production, while Life Cycle B (asynchronous) has the drug acting at cell infection. These two life cycles are chosen because they differ only in rate of rescue mutation $\nu(t)$ (both having $m_1 = 0$ and identical P_{pre}) and thus allow a more straightforward comparison.

We can visualize parameter effects through density plots of $P_{R\backslash P}$ (Figs. 6–8), here illustrated in the (u, s) plane. Darker shading represents higher values of $P_{R\backslash P}$, that is, greater importance of rescue. Two unequivocal effects are apparent. Firstly, asynchronicity between drug action and mutation always results in a larger contribution of rescue, as we would expect from the previous section. Visually, this is evident from a comparison of the top and bottom panels in Fig. 6, or of Figs. 7 and 8, showing corresponding results for Life Cycles A and B respectively. Secondly, the impact of drug efficacy ϵ is also obvious: increasing ϵ always decreases P'_{resc} without changing P_{pre}, and thus rescue is more important at low ϵ (Fig. 6).

The remaining parameter effects are less clear. In particular, R_0^0 affects the number and timing of de novo mutants during treatment in inconsistent directions, and the sensitivity of $p_{ext}(t)$ to R_0^0 across time is not straightforward. This feeds through to complicated effects on $P_{R\backslash P}$. We thus show plots across various R_0^0 values only to demonstrate robustness of other effects, without focussing on the impact of R_0^0 itself.

The other key parameters (u, s, and γ) each affect both P_{pre} and P'_{resc} in the same direction, yielding counteracting effects on $P_{R\backslash P}$. As a result, varying these parameters can have non-monotonic effects on $P_{R\backslash P}$. For instance, $P_{R\backslash P}$ will be zero at both very low mutation rates (such that $P_{pre} \approx P'_{resc} \approx 0$) and very high mutation rates (such that $P_{pre} \approx P'_{resc} \approx 1$), but generally non-zero in between. That is, as Figs. 7 and 8 indicate, rescue can be significant at some intermediate range of u.

The role of γ is more complicated. The probability of survival decreases at all times as γ increases, but this dependence is stronger at earlier times. (Note that the asymptotic value of $p_{ext}(t)$ is

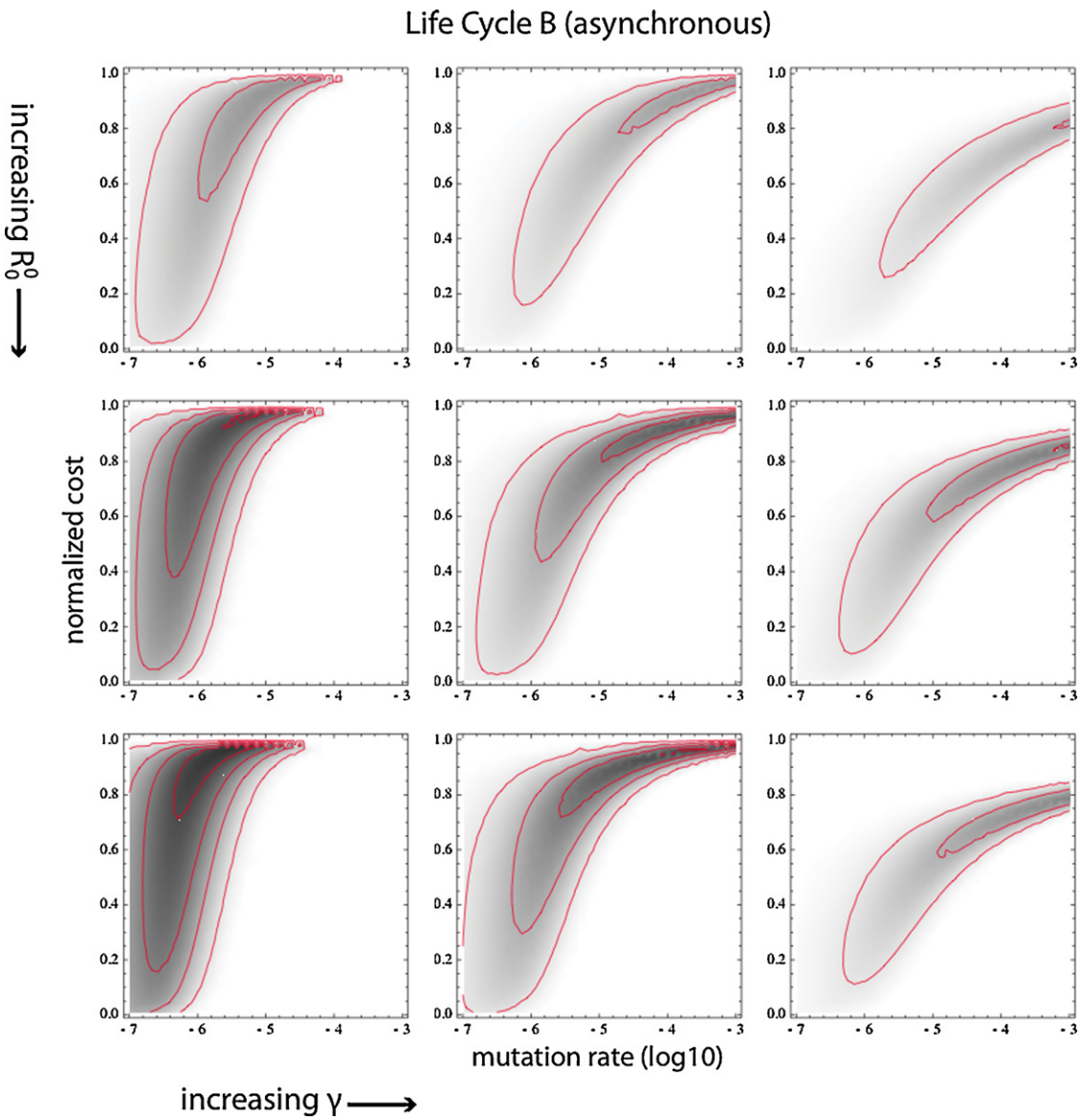

Fig. 8. Parameter effects on the relative importance of rescue, as measured by $P_{R\backslash P}$, in Life Cycle B. Shading and contours are the same as in Figs. 6 and 7, with parameter settings the same as in Figure 7.

independent of γ.) This incurs a relative disadvantage to mutants arising earlier, particularly those pre-existing. On the other hand, while increasing γ (with other parameters fixed) does not affect the number of pre-existing mutants, it reduces the number of mutants produced under treatment and tends to push this production earlier, incurring a relative disadvantage to rescue. Overall, then, increasing γ may either favour or disfavour rescue, depending on other parameter settings. Although increasing γ decreases $P_{R\backslash P}$ in the parameter region of Figs. 7 and 8, non-monotonic effects can be observed in other regions, as illustrated by density plots in the (u, γ) plane (Supplementary Figs. 3 and 4).

An overall study of the plots in Figs. 7 and 8, as well as Supplementary Figs. 3 and 4, suggests that rescue tends to make the most significant contribution when the cost of resistance is fairly high. This can be understood through the aforementioned dual disadvantage of cost incurred by pre-existing mutants. Whereas s does not affect the appearance of de novo mutants (for the life cycles under consideration), it decreases the number of pre-existing mutants, which have already faced selection in the pre-treatment environment. Furthermore, costly mutants face the greatest extinction risk early in treatment, when target cell levels are lowest. Nonetheless, $P_{R\backslash P}$ must necessarily drop off to zero at extremely high costs, for which survival is not possible (R_0^R drops below 1). The aforementioned factors suggest that, as s increases, it is P_{pre} that drops off before P'_{resc}, allowing an interval of relatively high cost at which rescue can make the major contribution to survival.

It is apparent that the key parameters show complex interaction effects. That is, for no parameter besides ϵ can we identify a directional effect on $P_{R\backslash P}$ that holds independently of other parameter settings. It is thus important to keep in mind that, although we have investigated the role of each parameter separately, there are likely to be correlations between their true values. For instance, relative infected cell death rate (γ) cannot increase indefinitely without reducing R_0^0. Certain interaction effects can be delineated. For instance, as u increases, the value of s maximizing $P_{R\backslash P}$ also increases (Figs. 7 and 8). This is because a larger number of mutants implies that both P_{pre} and P'_{resc} remain close to one over a larger range of s. That is, when the mutational influx is high, rescue only makes a difference for very costly mutants, but when mutations are rare, rescue can be significant even for lower cost mutants.

The increased complexity of parameter effects on the contribution of rescue in our model, compared to previous work (Ribeiro and Bonhoeffer, 2000), can in part be attributed to the measure of contribution we use. Since probabilities (unlike expected numbers) are constrained between 0 and 1, certain parameter effects saturate. That is, once there are so many mutants that survival is extremely likely (or so few that survival is extremely unlikely), pushing parameters further in the same direction makes a negligible difference. Furthermore, our consideration of stochastic extinctions during treatment impacts the findings. Since the cost of mutants affects their pre-treatment prevalence through selection, but does not affect their de novo appearance, neglecting cost-dependent extinctions during treatment gives a clear disadvantage to pre-existence, explaining the consistent directional effect of s found previously in the single-locus case (Ribeiro and Bonhoeffer, 2000). Stochastic losses also explain why we no longer find that increasing γ always favours pre-existence (Ribeiro and Bonhoeffer, 2000).

Waiting time for the emergence of resistance

For clinical reasons, we may be interested not only in the probability of resistance eventually emerging in a patient, but also in the time until this occurs. We may even anticipate being able to identify the source of resistance (pre-existence or rescue) based on the time at which resistance or viral rebound is detected. Analytically, we can derive the waiting time distribution for the first rescue mutant to appear (Supplementary Material), and this can indeed give some insight into one component of the overall waiting time. However, clinically, it is more relevant to consider the time until the total viral load rebounds to a detectable level. This is most easily investigated by simulation, since the analysis is complicated by multiple founders of mutant lineages and competition for target cells as the mutant population grows. We use a mock detection limit of 10^5 virions, which is 0.1% of the pre-treatment equilibrium number of virions, for illustration. (For comparison, the detection limit of a standard HIV assay is 50 copies per mL of plasma (Dornadula et al., 1999), whereas set-point viral loads mostly fall within the range of $10^{3.5}$ to $10^{5.5}$ copies per mL in peripheral blood (Fraser et al., 2007).)

By comparing simulated time courses of viral load dynamics under treatment (Supplementary Fig. 5), it turns out that there is not a large difference in the waiting time to detection, whether mutants are pre-existing or arise during treatment. Fig. 9 clearly shows the substantial overlap in the waiting time distributions for these two cases. This similarity can be explained by the relatively short waiting time for the first rescue mutant to appear (see Supplementary Material), combined with an initial decline in the pre-existing mutant population size as influx from wild type mutations is reduced while target cells have not yet rebounded sufficiently to support self-sustained mutant growth. That is, the time for mutant lineages to grow, rather than the time until lineages are founded, seems to dominate the overall waiting time until detection.

Nonetheless, we expect the degree of overlap of the waiting time distributions to be sensitive to parameter values. We thus investigate how the mean time of detection, provided resistance emerges, depends on drug efficacy ϵ, cost of resistance s, and mutation rate u (Supplementary Fig. 6). The waiting time turns out to be insensitive to ϵ, and shows little differentiation between pre-existence and rescue. Both these effects can be explained by the dominance of the mutant population growth phase – which is, to a good approximation, independent of the drug – in the overall waiting time. An observed increase in waiting time with s can primarily be explained by noting that a strain that replicates less efficiently takes a longer time to reach a given population size. The differentiation between pre-existence and rescue increases at low s because of the large difference in starting population size: for instance, at

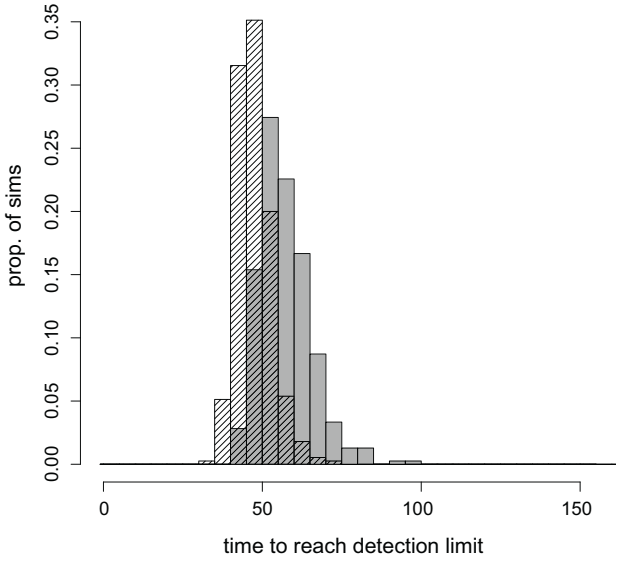

Fig. 9. Histogram of time on treatment until total viral load reaches the detection limit of 10^5. The distribution is derived from 390 simulation runs showing viral rebound in each case. Hatched: pre-existing mutants; grey: rescue mutants. We see the overlap in the darker regions. Simulations were performed for a life cycle with mutation at cell infection, cost at infectivity (β) of $s = 0.3$, and drug blocking cell infection with efficacy $\epsilon_I = 0.8$. (The simulations are the same as those in Supplementary Fig. 5.)

$s = 0.05$, there are on average 600 pre-existing mutants at the time treatment starts, versus zero rescue mutants. A similar effect occurs at high mutation rate. The waiting time under the rescue scenario declines slightly, due to the larger influx of de novo mutants; however, this is not as large as the decline of waiting time under the pre-existence scenario, in which the starting number of mutants increases substantially.

Overall, these results suggest that it may be difficult to infer whether outgrowth of resistance is due to pre-existing or rescue mutants. We expect the best possibility for differentiation to occur when the mutation rate is high and the cost of resistance is low: in this case, the large head start in population size gained by pre-existing mutants implies that the waiting time until reaching a detectable viral load tends to be lower. Although in some systems it may be possible to infer the source of resistance from the time at which viral load rebounds (Adiwijaya et al., 2010), in general we would proceed with caution in assuming that resistance that arises quickly is due to pre-existence.

Discussion

Resistance has repeatedly been observed to arise in patients infected with fast-evolving pathogens subjected to the strong selective pressure of drug treatment. The source of resistance – whether from genetic variation pre-existing in the pathogen population before drug treatment begins, or arising during ongoing replication under treatment – is an important line of investigation, both as a basic evolutionary problem and as an issue with clinical relevance for the optimal approach to treatment. Mathematical models play a key role in understanding the intra-host dynamics of the pathogen.

In this study, we have expanded the investigation of the sources of intra-host resistance to consider chronic viral pathogens with differing life cycles. Our aim was to better understand how we may or may not be able to generalize our understanding across diseases. We find that life cycle matters in a number of ways. Firstly, the mutational and cost mechanisms affect the mutation-selection balance reached before drug treatment begins. Mutants with defects

in persisting once generated will be present at lower frequencies than those with defects in producing offspring. Secondly, the mechanism of cost affects the chance that a mutant lineage survives, i.e. escapes stochastic extinction. In a scenario of increasing resources, corresponding to target cell rebound once the wild type is suppressed by drug treatment, we find that a mutant with a survival cost (i.e. increased death rate) is less likely to have descendants than a mutant with a productivity cost (i.e. decreased offspring production rate). This effect can be understood intuitively as an advantage to mutants that can "wait for better times ahead" to reproduce. We conjecture that, when resource availability affects "birth" rate, this may be a fairly general feature of stochastic demographic processes in an environment of increasing resources, whereas we would expect the opposite when resources are declining. (Note that our definition of cost across mechanisms implies that all mutants with a given magnitude of cost, s, have the same probability of stochastic extinction, namely $1/R_0^R = 1/(R_0^0(1-s))$, in a constant resource environment.) Thirdly, we find that the interaction between the step at which mutants are generated and the step at which the drug acts can have a major effect on the generation of rescue mutants once treatment begins. "Asynchronous" drugs, which block the opposite step to which mutations occur, leave a window of opportunity for existing sensitive-strain virus to undergo the mutant-generating step of its life cycle uninhibited, potentially producing virus which is subsequently resistant to the drug. This suggests that it is important to target the primary mutant-generating step of a virus's life cycle directly. We expect the precise effect of asynchronicity between drug action and mutation to be sensitive to model details, such as pharmacokinetics, outside our present scope. Nonetheless, asynchronicity can be relevant in real systems: for instance, there are sources of HIV virions (e.g. those associated with follicular dendritic cells) that do not clear fast (Blankson et al., 2002), and may thus represent a significant source of rescue mutations if drug treatment targets only virion production and not cell infection.

These findings join an emerging body of literature making the point that life cycle details matter. For instance, recent studies have explored how the mechanism of replication with mutation (Loverdo et al., 2012) and the timing of virion release over an infected cell's lifetime (Pearson et al., 2011) affect the fate of lineages. A common theme is that such details matter when stochastic effects are significant, as for an initially small population of a drug-resistant pathogen. Although already more general than previous modelling efforts in this area, our model is still restricted to "stamping machine" replication (Sanjuán et al., 2010), budding release of virions, and exponentially distributed infected cell lifetimes. Relaxing such assumptions is known to affect population dynamics (Lloyd, 2001; Heffernan and Wahl, 2005; Pearson et al., 2011). Indeed, the intricacies of viral life cycles and drug action may call for a yet more detailed examination on the intracellular level, with links to the intercellular level. Incorporating an intracellular description of HCV has already yielded novel insights into population dynamics (Guedj and Neumann, 2010). We expect further investigations along these lines, in directions of both greater generality and greater disease-specific detail, to continue painting a more nuanced picture of how life cycle details affect the emergence of resistance.

Through substantial analytical understanding of parameter dependencies, we were also able to identify regimes in which rescue plays a particularly important role in our system. Rescue tends to be most significant when drug efficacy is low and the cost of resistance is fairly high, mainly in agreement with previous findings specific to HIV (Ribeiro and Bonhoeffer, 2000), though with the caveat that neither rescue nor survival from pre-existence is possible once cost is too high. Since empirical observations suggest costs of resistance may indeed be high (see Supplementary Material), we would not downplay the importance of this parameter range. Furthermore, by explicitly considering probabilities of emergence instead of the proxy of expected numbers of mutants, the relative contribution of rescue may be considered largest at some intermediate range of total mutational influx, rather than independent of mutation rate (Ribeiro and Bonhoeffer, 2000). Our consideration of stochastic extinctions also enables us to say that rescue may be more important than previously thought, since mutants arising later during the course of target cell rebound have a better chance of survival. In particular, in contrast to earlier work (Ribeiro and Bonhoeffer, 2000), we predict that higher infected cell death rate does not always favour pre-existence. Indeed, there can be complex interaction effects among parameters.

Table 2
Comparison of parameter values across three important chronic viral diseases: human immunodeficiency virus (HIV), hepatitis B virus (HBV), and hepatitis C virus (HCV). Parameter estimates justifying these comparisons are provided in Supplementary Material.

Parameter	Comparison of diseases
Virion clearance rate, c	HIV > HCV > HBV
Uninfected cell death rate, d	HIV > HBV, HCV
Infected cell death rate, a	HIV > HCV > HBV
Relative infected cell death rate, γ	HCV > HIV, HBV
Basic reproductive number, R_0^0	HCV > HIV, HBV (?)
Pre-treatment infected cell population, y_S^*	HBV, HCV $\gg$ HIV
Drug efficacy, ϵ	Depends on the drug(s)
Mutation rate, u and cost, s	Depends on the per-base pair mutation rate, drug(s), genetic constraints, and mechanism of resistance

With our understanding of parameter dependencies, we can compare three important chronic viral diseases: HIV, HBV, and HCV. Table 2 summarizes how parameters vary across these diseases; see Supplementary Material for quantitative details and references. Interestingly, different factors act in different directions, such that no disease consistently appears more vulnerable to the emergence of resistance or more prone to a particular source. For instance, HCV has a larger infected cell population size than HIV, but also a higher relative infected cell death rate. We can also say that some of the differences observed among these diseases are unlikely to play a large role. For example, free virus clears more quickly in HIV than in HCV; however, independently of effects on R_0^0, we expect this distinction to be unimportant. Furthermore, large differences in infected cell death rate among the diseases are moderated by the fact that uninfected cell death rates follow a similar pattern. Of course, the speed with which resistance emerges in real time does depend on the absolute turnover rates, as measured by d. The intertwined influences of mutation rate and cost are more difficult to interpret. Available evidence indicates that the per-base pair mutation rate is fairly similar across these viruses. However, for any particular drug, the genetic basis of resistance (e.g. number of base changes required and number of possibilities yielding a resistant phenotype) and its phenotypic effects give rise to a particular effective mutation rate to the resistance allele and a particular cost. Furthermore, mutations may have pleiotropic effects, particularly when genes are encoded by overlapping reading frames, as in HBV, which may thus face more stringent constraints (Soriano et al., 2008). This could give rise to a lower effective (viable) mutation rate to resistance and/or higher costs. Finally, we note that some parameters, including viral set-point (pre-treatment population size) for HIV and infected cell lifetime for HBV, are known to vary widely across patients. This suggests that different patients with the same disease will be at varying risk for the emergence of resistance and the relative importance of rescue.

The source of drug resistance is difficult to investigate empirically, particularly in vivo, which is why mathematical modelling has

played such an important role in developing an understanding of this problem. Accordingly, it is difficult to test many of the detailed model results empirically. Nonetheless, our theoretical work suggests a few possibilities. One key prediction is that drug efficacy has very little effect on the probability or timing at which pre-existing drug-resistant mutants arise (in absolute numbers). This idea could perhaps be tested in an animal model by viral infection followed by treatment at varying drug dosages. If the emergence of resistance is independent of dose, it can likely be attributed to pre-existence. Conversely, however, an observed dependence may be explained not only by a predominant contribution of rescue, but also by mutants being only partially resistant. Another insight from our model relates to the time on treatment until resistance is detected. Our analysis of waiting times suggests that fast-emerging resistance cannot necessarily be attributed to pre-existence. We note, however, that our model assumes an idealized situation in which the drug(s) are effective at all times, in all anatomical compartments and cell types. Patient data at sufficient time resolution could indicate whether resistance actually emerges on a completely different time scale than our models predicts, which would indicate that other mechanisms, such as patient adherence issues or reservoirs of infected cells not responsive to drug, are important. Other infected cell populations could in principle also be analysed by our model, so long as they are declining, even if slowly. Indeed, we expect that such populations could make a disproportionate contribution to rescue, since mutants arising later face a more favourable level of target cells. Naturally, we would also expect factors such as the activation of latently infected cells in HIV to add an ongoing source of rescue at a low rate. In a complementary approach, another recent study considered these long-term sources but neglected the dynamic short-term decline phase of the drug-sensitive population (Pennings, 2012).

Our results also have significance for researchers interested in using theory to develop more accurate quantifications, and suggest directions for further empirical work in vitro. Our model elucidates which parameters are most important to measure in order to better predict the emergence of drug resistance. We also point out when a detailed understanding of life cycle is significant. For instance, it is important to identify the step(s) of the life cycle affected by costly resistance, not only the impact on an overall measure of fitness. This is particularly significant if estimated fitness costs are high. We also caution that mutation rate estimates obtained from frequency measurements at the mutation-selection balance may be affected by the mechanism of cost; specifically, the mutation rate may be underestimated if costs are borne in part by reduced survival instead of productivity.

Returning to a more general theoretical context, understanding the source of intra-host emergence of resistance remains an important question across diseases, not only chronic viral infections. Interestingly, there have been a few convergent results in very different models, besides those presented here and previously for viral pathogens. A study of resistance to targeted chemotherapy in cancerous tumours concluded that pre-existence was more likely than rescue, except in the unrealistic case of a single, very ineffective drug (Komarova and Wodarz, 2005); no cost of resistance was incorporated here. A more generic model (Orr and Unckless, 2008) described a population declining in size following an environmental change that reduces the fitness of the wild type, with the possibility of rescue through outgrowth of a variant more fit in the new environment. "Standing genetic variation" (analogous to pre-existing mutants) was the more likely source of rescue than mutants arising after the environmental change, provided the deleterious effect of this mutation before the change was sufficiently small (Orr and Unckless, 2008). These parallel conclusions motivate further investigation into their generality and possible exceptions.

To this end, the mathematical machinery developed here for analytical approximations could be more broadly useful in exploring various life cycles and even different diseases, as the general techniques are widely transferable. Some extensions, such as incorporating partial resistance or differing costs in the presence or absence of drug, would be straightforward to incorporate into our model. Others, such as time-varying drug efficacy (due to pharmacokinetics and therapy adherence patterns) and multiple mutational steps (including primary resistance to multiple drugs, as well as compensatory mutations), will require larger extensions. Incorporating non-equilibrium dynamics, as in acute infections or slow-turnover cellular compartments, remains challenging. Acute infections, such as influenza, have the further complication that the time varying nature of the immune response, which ultimately leads to clearance even without drug treatment, cannot be neglected. However, we expect our mathematical approach to transfer readily to other diseases in which dynamics have equilibrated before treatment begins, and in which resistance subsequently emerges stochastically in an environment of possibly changing resource availability. In this way we can gain some analytical understanding of parameter dependencies in the system, and hence insight into the important factors driving the emergence of drug resistance.

Acknowledgments

The authors wish to thank members of the Theoretical Biology group at ETH Zürich, particularly the drug resistance discussion group, Roland Regös, and Tanja Stadler, for helpful discussion; Ruy Ribeiro, for providing a copy of his PhD thesis; and Jamie Lloyd-Smith and two anonymous reviewers, for useful comments which helped us to strengthen this manuscript. This research was supported in part by the European Research Council under the 7th Framework Programme of the European Commission ("PBDR": Grant Agreement Number 268540). H.K.A. is funded in part by a postgraduate scholarship from the Natural Sciences and Engineering Research Council of Canada. The authors also gratefully acknowledge support from the ETH Zürich. These funding sources had no involvement in the design, analysis, or writing of this study.

Appendix A. Supplementary data

Supplementary data associated with this article can be found, in the online version, at http://dx.doi.org/10.1016/j.epidem.2012.10.001.

References

Adiwijaya, B.S., Herrmann, E., Hare, B., Kieffer, T., Lin, C., Kwong, A.D., Garg, V., Randle, J.C.R., Sarrazin, C., Zeuzem, S., Caron, P.R., 2010. A multi-variant, viral dynamic model of genotype 1 HCV to assess the in vivo evolution of protease-inhibitor resistant variants. PLOS Computational Biology 6, e1000745.

Bell, G., Gonzalez, A., 2009. Evolutionary rescue can prevent extinction following environmental change. Ecology Letters 12, 942–948.

Blankson, J.N., Persaud, D., Siliciano, R.F., 2002. The challenge of viral reservoirs in HIV-1 infection. Annual Review of Medicine 53, 557–593.

Bonhoeffer, S., May, R.M., Shaw, G.M., Nowak, M.A., 1997. Pre-existence and emergence of drug resistance in HIV-1 infection. Proceedings of the Royal Society: Biological Sciences 264, 631–637.

Bonhoeffer, S., Nowak, M.A., 1997. Pre-existence and emergence of drug resistance in HIV-1 infection. Proceedings of the Royal Society: Biological Sciences 264, 631–637.

Coffin, J.M., 1995. HIV population dynamics in vivo: implications for genetic variation, pathogenesis, and therapy. Science 267, 483–489.

Dahari, H., Lo, A., Ribeiro, R.M., Perelson, A.S., 2007. Modeling hepatitis C virus dynamics: liver regeneration and critical drug efficacy. Journal of Theoretical Biology 247, 371–381.

Dornadula, G., Zhang, H., VanUitert, B., Stern, J., Livornese, L., Ingerman, M.J., Witek, J., Kedanis, R.J., Natkin, J., DeSimone, J., Pomerantz, R.J., 1999. Residual HIV-1 RNA in blood plasma of patients taking suppressive highly active antiretroviral therapy. The Journal of the American Medical Association 282, 1627–1632.

Fraser, C., Hollingsworth, T.D., Chapman, R., de Wolf, F., Hanage, W.P., 2007. Variation in HIV-1 set-point viral load: epidemiological analysis and an evolutionary hypothesis. Proceedings of the National Academy of Sciences of the United States of America 104, 17441–17446.

Gadhamsetty, S., Dixit, N.M., 2010. Estimating frequencies of minority nevirapine-resistant strains in chronically infected HIV-1-infected individuals naïve to nevirapine by using stochastic simulations and a mathematical model. Journal of Virology 84, 10230–10240.

Ganem, D., Schneider, R.J., 2001. Hepadnaviridae: the viruses and their replication. In: Knipe, D.M., Howley, P.M. (Eds.), In: Fields Virology, 4th ed., vol. 2. Lippincott Williams & Wilkins, Philadelphia, USA, pp. 2923–2969 (Chapter 86).

Goff, S.P., 2001. Retroviridae: the retroviruses and their replication. In: Knipe, D.M., Howley, P.M. (Eds.), In: Fields Virology, 4th ed., vol. 2. Lippincott Williams & Wilkins, Philadelphia, USA, pp. 1871–1939 (Chapter 57).

Goldberg, D.E., Siliciano, R.F., Jacobs Jr., W.R., 2012. Outwitting evolution: fighting drug-resistant TB, malaria, and HIV. Cell 148, 1271–1283.

Guedj, J., Neumann, A.U., 2010. Understanding hepatitis C viral dynamics with direct-acting antiviral agents due to the interplay between intracellular replication and cellular infection dynamics. Journal of Theoretical Biology 267, 330–340.

Guedj, J., Rong, L., Dahari, H., Perelson, A.S., 2010. A perspective on modelling hepatitis C virus infection. Journal of Viral Hepatitis 17, 825–833.

Heffernan, J.M., Wahl, L.M., 2005. Monte Carlo estimates of natural variation in HIV infection. Journal of Theoretical Biology 236, 137–153.

Hirsch, M.S., Günthard, H.F., Schapiro, J.M., Brun-Vézinet, F., Clotet, B., Hammer, S.M., Johnson, V.A., Kuritzkes, D.R., Mellors, J.W., Pillay, D., Yeni, P.G., Jacobsen, D.M., Richman, D.D., 2008. Antiretroviral drug resistance testing in adult HIV-1 infection: 2008 recommendations of an International AIDS society – USAA panel. Clinical Infectious Diseases 47, 266–285.

Johnson, V.A., Calvez, V., Günthard, H.F., Paredes, R., Pillay, D., Shafer, R., Wensing, A.M., Richman, D.D., 2011. 2011 update of the drug resistance mutations in HIV-1. Topics in Antiviral Medicine 19, 156–164.

Kendall, D.G., 1949. Stochastic processes and population growth. Journal of the Royal Statistical Society: Series B (Methodology) 11, 230–282.

Komarova, N.L., Wodarz, D., 2005. Drug resistance in cancer: principles of emergence and prevention. Proceedings of the National Academy of Sciences of the United States of America 102, 9714–9719.

Lindenbach, B.D., Rice, C.M., 2001. Flaviviridae: the viruses and their replication. In: Knipe, D.M., Howley, P.M. (Eds.), In: Fields Virology, 4th ed, vol. 1. Lippincott Williams & Wilkins, Philadelphia, USA, pp. 991–1041 (Chapter 32).

Lloyd, A.L., 2001. The dependence of viral parameter estimates on the assumed viral life cycle: limitations of studies of viral load data. Proceedings of the Royal Society B: Biological Sciences 268, 847–854.

Loverdo, C., Park, M., Schreiber, S.J., Lloyd-Smith, J.O., 2012. Influence of viral replication mechanisms on within-host evolutionary dynamics. Evolution 66, 3462–3471.

Mansky, L.M., Temin, H.M., 1995. Lower in vivo mutation rate of human immunodeficiency virus type 1 than that predicted from the fidelity of purified reverse transcriptase. Journal of Virology 69, 5087–5094.

Nowak, M.A., Bonhoeffer, S., Hill, A.M., Boehme, R., Thomas, H.C., McDade, H., 1996. Viral dynamics in hepatitis B infection. Proceedings of the National Academy of Sciences of the United States of America 93, 4398–4402.

Nowak, M.A., May, R.M., 2000. Virus Dynamics. Oxford University Press, Oxford, UK.

Orr, H.A., Unckless, R.L., 2008. Population extinction and the genetics of adaptation. The American Naturalist 172, 160–169.

Parzen, E., 1999. Stochastic Processes. SIAM, Philadelphia, PA, USA.

Pearson, J.E., Krapivsky, P., Perelson, A.S., 2011. Stochastic theory of early viral infection: continuous versus burst production of virions. PLOS Computational Biology 7, e1001058.

Pennings, P.S., 2012. Standing genetic variation and the evolution of drug resistance in HIV. PLOS Computational Biology 8, e1002527.

Perelson, A.S., 2002. Modelling viral and immune system dynamics. Nature Reviews Immunology 21, 28–36.

Ribeiro, R.M., 1999. Models of viral diversity and disease development in HIV infection. Ph.D. thesis. University of Oxford. Oxford, UK.

Ribeiro, R.M., Bonhoeffer, S., 1999. A stochastic model for primary HIV infection: optimal timing of therapy. AIDS 13, 351–357.

Ribeiro, R.M., Bonhoeffer, S., 2000. Production of resistant HIV mutants during antiretroviral therapy. Proceedings of the National Academy of Sciences of the United States of America 97, 7681–7686.

Ribeiro, R.M., Bonhoeffer, S., Nowak, M.A., 1998. The frequency of resistant mutant virus before antiviral therapy. AIDS 12, 461–465.

Ribeiro, R.M., Lo, A., Perelson, A.S., 2002. Dynamics of hepatitis B virus infection. Microbes and Infection 4, 829–835.

Roberts, D.E., Ribeiro, R.M., 2001. Comparison of different treatment regimens for the emergence of new resistance under therapy. Journal of Acquired Immune Deficiency Syndromes 27, 331–335.

Rong, L., Dahari, H., Ribeiro, R.M., Perelson, A.S., 2010. Rapid emergence of protease inhibitor resistance in hepatitis C virus. Science Translational Medicine 2, 1–9, 30ra32.

Rong, L., Feng, Z., Perelson, A.S., 2007. Emergence of HIV-1 drug resistance during antiretroviral treatment. Bulletin of Mathematical Biology 69, 2027–2060.

Sanjuán, R., Nebot, M.R., Chirico, N., Mansky, L.M., Belshaw, R., 2010. Viral mutation rates. Journal of Virology 84, 9733–9748.

Shiri, T., Welte, A., 2011. Modelling the impact of acute infection dynamics on the accumulation of HIV-1 mutations. Journal of Theoretical Biology 279, 44–54.

Soriano, V., Perelson, A.S., Zoulim, F., 2008. Why are there different dynamics in the selection of drug resistance in HIV and hepatitis B and C viruses? Journal of Antimicrobial Chemotherapy 62, 1–4.

Wilf, H.S., 1994. Generatingfunctionology, 2nd ed. Academic Press Inc, Internet Edition.